[3]Igra, O., Ben-Dor, G., Aizik, F., and Gelfand, B., "Experimental and Numerical Investigation of Shock Wave Attenuation in Dust-Gas Suspensions," *Proceedings of the 19th International Symposium on Shock Tubes and Waves* (Marseille, France), Springer, Germany, 1993, pp. 49–54.

[4]Olim, M., Igra, O., Mond, M., and Ben-Dor, G., "A General Attenuation Law of Moderate Planar Shock Waves Propagating into Dusty Gases," *Proceedings of the 18th International Symposium on Shock Tubes and Waves*, Springer–Verlag, New York, 1991, pp. 217–225.

[5]Aizik, F., Ben-Dor, G., Elperin, T., Igra, O., Mond, M., and Gronig, H., "Attenuation Law of Planar Shock Waves Propagating Through Dust-Gas Suspensions," *AIAA Journal*, Vol. 33, No. 5, 1995, pp. 953–955.

G. Laufer
Associate Editor

Effect of Loading Parameters on Damage-Induced Shear-Extension Coupling in Laminate

Y. A. Dzenis*
University of Nebraska, Lincoln, Nebraska 68588-0347
and
S. P. Joshi†
University of Texas at Arlington, Arlington, Texas 76019

Introduction

MATERIAL anisotropy is an important issue in composite structural design. It was shown in Refs. 1 and 2 that shear-extension coupling can appear in an initially balanced laminate due to unequal damage accumulation in plies with opposite orientation under the shear loading and that this may result in significant reduction of laminate shear strength. The effects of intrinsic factors such as angle-ply orientation and the presence of 0-deg plies on damage-induced anisotropy in laminates are studied in Ref. 3. The objective of this Note is to investigate the effects of extrinsic factors, i.e., the combination of shear and tensile/compressive loading as well as loading rate and deviation.

A stochastic damage accumulation model developed in Refs. 1 and 2 is used in the analysis. Random quasistationary in-plane loading is defined as a Gaussian process with autocorrelation time τ_0 and standard deviation σ_i. Stochastic function theory, the theory of excursions of random process beyond the limits as a strain failure criterion, is applied to estimate the probabilities of failure in plies. Three modes of failure, i.e., fiber breakage, matrix transverse failure, and matrix or interface shear cracking, are taken into account. Calculated probabilities are utilized in reducing ply stiffness. A brief description of the mathematical formulation of the model is given in the following paragraphs. The detailed model description is presented in Refs. 1 and 2.

Consider an orthotropic laminated composite consisting of unidirectionally reinforced plies with initial stochastic elastic material properties $\tilde{E}^k_{1_0}$, $\tilde{E}^k_{2_0}$, $\tilde{G}^k_{12_0}$, $\tilde{\nu}^k_{12_0}$. Index k denotes the ply number. Laminate lay up is described by ply orientation angles α^k and ply thicknesses h^k. Load increment applied to a laminate results in a random stress–strain field in each ply. Even at very low levels of applied load, a nonzero probability of ply failure exists and damages start to accumulate in the composite. Accumulation of damages causes a reduction in laminate stiffness and a redistribution of stresses among plies.

Received Dec. 15, 1995; revision received Oct. 9, 1996; accepted for publication Dec. 26, 1996; also published in *AIAA Journal on Disc*, Volume 2, Number 2.

*Assistant Professor, Department of Engineering Mechanics. Member AIAA.

†Professor, Center for Composite Materials, Department of Mechanical and Aerospace Engineering. Member AIAA.

Assume that in-plane stresses applied to a composite are monotonically increasing functions of a parameter t, $\bar{\sigma}_i(t) = [\sigma_{11}(t), \sigma_{22}(t), \sigma_{12}(t)]$, with parametric derivatives $\dot{\bar{\sigma}}_i(t)$. Random deformations of the composite then can be calculated by using integral equations:

$$\tilde{\varepsilon}_i(t) = \int_0^t \tilde{S}_{ij}(\tau)\dot{\sigma}_j(\tau)\mathrm{d}\tau \tag{1}$$

where $\tilde{S}_{ij}$ are current effective laminate compliances. They depend on lamina current elastic properties and composite lay up:

$$\tilde{S}_{ij}(\tau) = L\left[\tilde{E}^k_1(\tau), \tilde{E}^k_2(\tau), \tilde{G}^k_{12}(\tau), \tilde{\nu}^k_{12}(\tau), \alpha^k\right] \tag{2}$$

The current elastic constants of plies are functions of the initial elastic constants and the current damage functions:

$$\tilde{E}^k_1(\tau), \tilde{E}^k_2(\tau), \tilde{G}^k_{12}(\tau), \tilde{\nu}^k_{12}(\tau) = M\left[\tilde{E}^k_{1_0}, \tilde{E}^k_{2_0}, \tilde{G}^k_{12_0}, \tilde{\nu}^k_{12_0}, r^k_i(\tau)\right] \tag{3}$$

Damage functions may be calculated by using ply random stress–strain field parameters and some appropriate failure criteria:

$$r^k_i(\tau) = R\left[\tilde{\varepsilon}^k_i(\tau), \tilde{\sigma}^k_i(\tau)\right] \tag{4}$$

Ply stress–strain field parameters are calculated, in turn, from known composite strains $\tilde{\varepsilon}_i$ [Eq. (1)]:

$$\begin{aligned} \tilde{\varepsilon}^k_i(\tau) &= K\left[\tilde{\varepsilon}_i(\tau), \alpha^k\right] \\ \tilde{\sigma}^k_i(\tau) &= P\left[\tilde{\varepsilon}^k_i(\tau), \tilde{E}^k_1(\tau), \tilde{E}^k_2(\tau), \tilde{G}^k_{12}(\tau), \tilde{\nu}^k_{12}(\tau)\right] \end{aligned} \tag{5}$$

L, M, R, K, and P are stochastic functional operators to be specified. According to this approach, current composite elastic properties and, therefore, composite deformations and damage functions are dependent on loading history. To integrate Eq. (1), we need to calculate the stochastic stress–strain field that depends on the stochastic material properties and the deformation history. The failure criterion [Eq. (4)] should be chosen to obtain damage functions. The stiffness reduction algorithm due to damage accumulation in plies [Eq. (3)] has to be specified. The failure criterion and the stiffness reduction algorithm are described in Ref. 1.

A numerical algorithm and computer code for damage evolution and deformation history prediction in laminates subjected to general in-plane loading are developed in *Mathematica*®. In this Note, the model mentioned earlier is applied to analyze the behavior of $[\pm 30]_s$ Kevlar®/epoxy laminate under combined shear and tension/compression at various loading rates and deviations. The properties of the unidirectional Kevlar/epoxy lamina used in the calculations are given in Ref. 1.

Results and Discussion

Results of analysis of the effect of shear load in conjunction with longitudinal in-plane loading on damage-induced shear-extension coupling are shown in Tables 1–3. Table 1 corresponds to combined shear/tension $\{\sigma_{xx}, 0, \tau_{xy}\}$, Table 2 corresponds to combined shear/compression $\{-\sigma_{xx}, 0, \tau_{xy}\}$, and Table 3 corresponds to combined shear/biaxial tension $\{\sigma_{xx}, \sigma_{yy} = \sigma_{xx}, \tau_{xy}\}$. The A_{16}/A_{66} and A_{26}/A_{66} variables represent maximal relative shear-extension coupling coefficients of the in-plane stiffness matrix of laminate at failure, and S_{xy} and S^l_{xy} correspond to laminate average shear stress at failure calculated with and without taking into account damage-induced anisotropy, respectively. The final laminate failure corresponds to the shear stress when any one of the apparent moduli of the laminate becomes vanishingly small. The shear strength of the angle-ply laminate, S_{xy}, obtained by using the maximum strain criterion, is also included for reference. The ply-by-ply failure procedure described in Ref. 4 is utilized for calculating S_{xy}. The laminate is assumed to be failed when fiber and matrix in each ply is failed according to the maximum strain criterion. Note that the direct comparison between the strength prediction by the model (S_{xy} and S^l_{xy}) and the maximum strain criterion ($\hat{S}_{xy}$) is not possible because the effect of the loading rate cannot be accounted for in the maximum strain criterion. Obviously, the strengths are higher at the higher loading rates.[1]

Table 1 Variation of shear-extension coupling coefficients and shear stress at failure of $[\pm 30]_s$ laminate with the ratio of longitudinal to shear loading: combined tension/shear

σ_{xx}/τ_{xy}	A_{16}/A_{66}	A_{26}/A_{66}	S_{xy}, MPa	Sl_{xy}, MPa	$\hat{S}_{xy}$, MPa
0	1.59	0.53	225	335	163
0.1	1.57	0.51	230	335	174
0.2	1.56	0.53	240	340	188
0.4	1.51	0.55	250	330	212
0.6	1.45	0.53	255	275	248
0.8	1.21	0.44	245	245	223
1.0	0.71	0.26	220	220	190

Table 2 Variation of shear-extension coupling coefficients and shear stress at failure of $[\pm 30]_s$ laminate with the ratio of longitudinal to shear loading: combined compression/shear

$-\sigma_{xx}/\tau_{xy}$	A_{16}/A_{66}	A_{26}/A_{66}	S_{xy}, MPa	Sl_{xy}, MPa	$\hat{S}_{xy}$, MPa
0	1.59	0.53	225	335	163
0.1	1.58	0.49	215	340	155
0.2	1.59	0.48	210	350	144
0.4	1.58	0.47	195	335	129
0.6	1.59	0.47	185	240	156
0.8	1.58	0.48	175	195	156
1.0	1.56	0.48	165	170	156

Table 3 Variation of shear-extension coupling coefficients and shear stress at failure of $[\pm 30]_s$ laminate with the ratio of longitudinal to shear loading: combined biaxial tension/shear

$\sigma_{xx}/\tau_{xy} = \sigma_{yy}/\tau_{xy}$	A_{16}/A_{66}	A_{26}/A_{66}	S_{xy}, MPa	Sl_{xy}, MPa	$\hat{S}_{xy}$, MPa
0	1.59	0.53	225	335	163
0.1	1.59	0.49	230	345	170
0.2	1.59	0.47	235	320	156
0.4	1.25	0.39	195	200	156
0.6	0.51	0.16	150	155	156
0.8	0.24	0.07	125	125	156
1.0	0.15	0.05	110	110	156

Table 4 Variation of shear-extension coupling coefficients at failure and strength of $[\pm 30]_s$ laminate with shear stress deviation; loading rate is 1 MPa/τ_0

σ_q, MPa	A_{16}/A_{66}	A_{26}/A_{66}	S_{xy}, MPa	Sl_{xy}, MPa
0.1	1.61	0.49	225	443
1	1.59	0.47	198	355
5	1.60	0.47	155	250
10	1.54	0.51	75	108
15	1.20	0.40	43	45

Shear loading rate in all cases is 10 MPa/τ_0, and the loading deviation of all nonzero components is 10 MPa. Analysis shows that application of tensile loading in addition to shear loading (Table 1) causes no remarkable effect on maximal coupling at failure for loading ratios σ_{xx}/τ_{xy} lower than 0.6; however, combined tension and shear reduces the coupling for higher ratios. Laminate shear strength S_{xy} is maximal at a loading ratio of about 0.6. The effect of damage-induced coupling on shear strength is observed for loading ratios below 0.6. Combining compression and shear (Table 2) does not change maximal coupling significantly in the interval of load ratios being investigated. The shear strength S_{xy} almost monotonically reduces with growing $-\sigma_{xx}/\tau_{xy}$. The effect of coupling on shear strength exhibits a maximum at $-\sigma_{xx}/\tau_{xy} = 0.2$, and Sl_{xy} is 72% higher than S_{xy} at this loading ratio. The behavior of laminate under combined shear/biaxial tension (Table 3) is similar to that under tension (Table 1); however, coupling reduction starts at lower longitudinal/shear stress ratios.

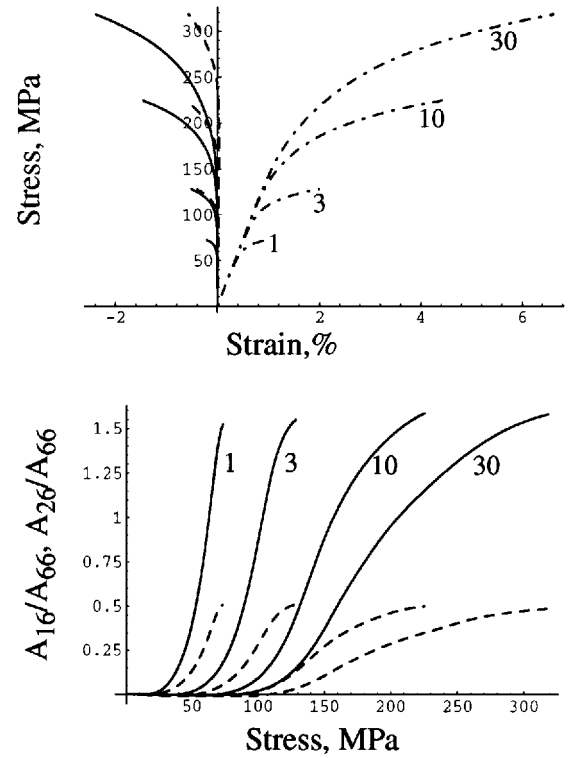

Fig. 1 a) Stress–strain diagram and b) variation of shear-extension coupling coefficients in $[\pm 30]_s$ laminate under shear. Numbers indicate loading rate in MPa/τ_0, loading deviation σ_q = 10 MPa.

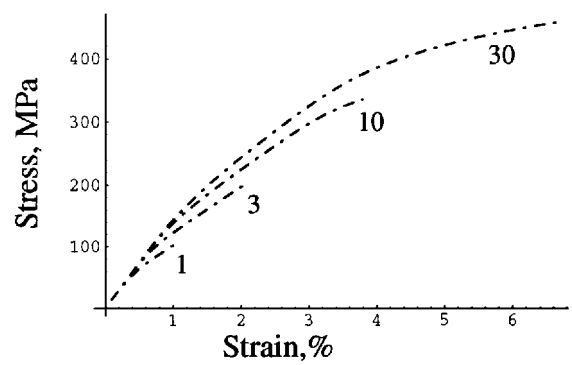

Fig. 2a Shear stress–strain plots calculated without accounting for damage-induced anisotropy in $[\pm 30]_s$ laminate under shear. Numbers indicate loading rate in MPa/τ_0, loading deviation σ_q = 10 MPa.

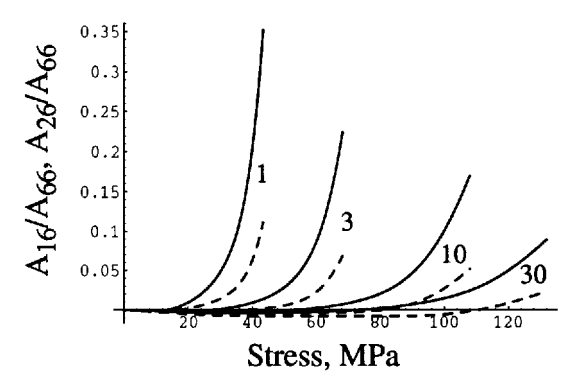

Fig. 2b Variation of shear-extension coupling coefficients in $[\pm 30]_s$ laminate under complex in-plane loading. Numbers indicate loading rate in MPa/τ_0, loading deviation σ_q = 10 MPa.

The shear loading initially causes matrix damage, followed by fiber failures in the ply experiencing compression in the fiber direction. The orthotropy in material properties decreases in this ply relative to the other ply, creating shear-extension coupling. This results in further fiber damage in the ply and an eventual decrease in the final failure load. The results presented in Tables 1–3 corroborate this physical reasoning. The fiber damage produced by the damage-induced anisotropy is a small fraction of the fiber damage produced by the applied tension/compression loading for cases with high ratios of tension/compression to shear loading. For ratios greater than about 0.5, the difference between S_{xy} and S'_{xy} is relatively small, as one would expect.

The effects of loading rate on laminate behavior are shown in Figs. 1 and 2. Predicted stress–strain curves of $[\pm 30]_s$ laminate under shear for four loading rates are shown in Fig. 1a (solid, dashed, and dot–dashed lines correspond to ε_{xx}, ε_{yy}, and γ_{xy}, respectively). Variation of relative shear-extension coupling coefficients is shown in Fig. 1b (solid lines, A_{16}; dashed lines, A_{26}). The increase in loading rate substantially increases the strength of the laminate (see discussion in Ref. 1), but the values of A_{16}/A_{66} and A_{26}/A_{66} ratios at failure are independent of the loading rate. Comparisons with stress–strain diagrams predicted without accounting for damage-induced anisotropy (Fig. 2a) show that the effect of the damage-induced coupling on the shear strength is nearly independent of stress rate. However, variation of coupling coefficients under complex in-plane loading $\sigma_{xx} = \sigma_{yy} = \tau_{xy} = \sigma$ (Fig. 2b) depends on the stress rate. The coupling is lower at high loading rates.

The effect of stress deviation on damage-induced anisotropy in laminate under shear (Table 4) shows that maximal coupling at failure starts to be reduced at deviations higher than 10 MPa. The damage-induced coupling significantly decreases shear strength at low deviations. For example, neglecting damage-induced anisotropy almost doubles the estimate of shear strength at $\sigma_q = 0.1$ MPa.

Conclusions

The shear-extension coupling due to damage in an initially balanced $[\pm 30]_s$ laminate was studied using a damage evolution model developed by the authors. The effects of complex loading application and loading rate and deviation were investigated. It was shown that the combination of shear loading with uniaxial or biaxial tension and compression reduces shear-extension coupling when the longitudinal-to-shear-loading ratio is sufficiently high. Damage-induced shear-extension coupling is more pronounced at low loading deviations.

The analysis shows that neglecting damage-induced coupling, as most existing models do, may lead to substantial overestimation of the laminate strength. The overestimation by not taking into account the damage-induced anisotropy is severe for loads with a low deviation and predominantly shear loads. The cases studied in this Note clearly bring out the shortcoming of models that do not take into account the damage-induced anisotropy, especially when damage is slowly progressing. The effect of loading rate on angle-ply laminate was compared with previous experimental observations. Experiments studying the effect of all of the parameters discussed in this Note are not available in the open literature. The authors plan to carry out such experiments in the future to verify the predictive capabilities of the analytical model.

References

[1] Dzenis, Y. A., Joshi, S. P., and Bogdanovich, A. E., "Behavior of Laminated Composites Under Monotonically Increasing Random Load," *AIAA Journal*, Vol. 31, No. 12, 1993, pp. 2329–2334.

[2] Dzenis, Y. A., Joshi, S. P., and Bogdanovich, A. E., "Damage Evolution Modeling in Orthotropic Laminated Composites," *AIAA Journal*, Vol. 32, No. 2, 1994, pp. 357–364.

[3] Dzenis, Y. A., and Joshi, S. P., "Damage Induced Anisotropy in Laminates," *Advanced Composites Letters*, Vol. 2, No. 3, 1993, pp. 97–99.

[4] Agarwal, B. D., and Broutman, L. J., *Analysis and Performance of Fiber Composites*, Wiley, New York, 1980, Chaps. 4 and 6.

R. K. Kapania
Associate Editor

Simplified Method for Predicting Onset of Open-Mode Free Edge Delamination

J. X. Tao* and C. T. Sun†
Purdue University, West Lafayette, Indiana 47907-1282

Introduction

INTERLAMINAR stresses in composite laminates are caused by the mismatch in material properties of the constituent laminas and the stacking sequence.[1] Several methods are available for analyzing interlaminar stresses at free edges. These include the finite element method,[2] complex stress potential method,[3] and variational approach.[4] These solution procedures are all quite involved.

The interlaminar normal stress is caused by the mismatch in Poisson's ratios of the constituent laminas. The problem of predicting interlaminar normal stress and the influence of stacking sequence on laminate strength was discussed by Pagano and Pipes.[5,6] An approximate distribution of interlaminar normal stress at the free edge of a laminate in uniform axial strain was assumed based on the moment equilibrium of the upper sublaminate. Herakovich[1] discussed the relationship between engineering properties and delamination of composite materials. Interface moment was related to the resistance of the laminate to open-mode delamination. However, no equation describing this relation has been devised.

In this study, an attempt was made to relate average interlaminar normal stress to interface moment at the free edge for several families of laminates. By establishing a relation between these two variables, the average interlaminar normal stress was obtained by the classical laminated plate theory (CLPT). The relation was then used to predict the onset of open-mode free edge delamination for three laminates. The method was verified by comparing the predictions with existing experimental data.

Preliminary Consideration

Consider a balanced and symmetric laminate subjected to uniform axial extension along the x direction (Fig. 1). For a long laminate, the state of stress can be regarded as independent of the longitudinal direction, thus reducing the problem to a pseudo-three-dimensional problem.

The stress state in a sublaminate above the kth interface is illustrated in Fig. 2. Because of the mismatch in Poisson's ratios of the individual layers, transverse stresses σ_y are induced in these layers. The magnitudes and signs of these stresses depend only on the mismatch of the Poisson's ratios and can be determined by CLPT. They are independent of the stacking sequence. The equilibrium of this sublaminate in the y direction requires that $\tau^k_{yz}(y)$ be developed at the interface to balance the transverse stress. Moment equilibrium about the x axis requires that $\sigma^k_z(y)$ be developed at the interface; $\sigma^k_z(y)$ must be self-equilibrating, and its distribution must be equivalent to a couple of on-zero moments when equilibrium in the z direction is considered. Thus, interlaminar normal stress $\sigma^k_z(y)$ can be related to the in-plane transverse stresses $\sigma^i_y (i = 1, 2, \ldots, k)$ through

$$\int_0^b \sigma^k_z(y)\, y\, \mathrm{d}y = \sum_i^k \sigma^i_y h_i \left(\frac{z_i + z_{i-1}}{2} - z_k \right) = m^{(k)} \qquad (1)$$

Received June 3, 1996; revision received Nov. 18, 1996; accepted for publication Nov. 23, 1996; also published in *AIAA Journal on Disc*, Volume 2, Number 2.

*Graduate Student, School of Aeronautics and Astronautics; currently Project Engineer, Delphi Chassis Systems, General Motors, Dayton, OH 45401.

†Professor, School of Aeronautics and Astronautics. Fellow AIAA.